THERMAL DECOMPOSITION BEHAVIOUR OF NATURAL BASTNASITE CRYSTAL IN CALCINATION①

Xiang, Jun Zhang, Chengxiang Tu, Ganfeng Ren, Chengzhi
Department of Nonferrous Metals Metallurgy,
Northeastern University, Shenyang 110006

ABSTRACT

The thermal decomposition behaviour of natural bastnasite crystal, mined from Mianning, Sichuan province, in calcination in air was studied by DTA, TG, XRD and chemical analysis methods. The decomposition procedure can be separated into two steps. At first, (Ce, La)CO_3F is oxidized and decomposed into (Ce, La)$O_{1+x}F_{1-x}$ at lower temperature. When calcination temperature and time increase, (Ce, La)$O_{1+x}F_{1-x}$ is farther oxidized and decomposed. The final products are CeO_2 and other rare earth compounds. Part of F is lost during the calcination procedure, but not for Si. The total weight lost is 17.095%. The activation energy E of the calcination reaction is 49.325 kJ/mol and the reaction order n is 1.123 by thermal dynamic calculation.

Key words: bastnasite calcination thermal dynamic calculation

1 INTRODUCTION

Bastnasite is one of the most valuable rare earth ores in industry. During the industry processing, it is calcined more frequently now[1~3]. There were only a limited number of studies about the calcination process of the bastnasite[1, 4, 5]. But they were mainly on the chemical and optical properties of the calcination products of the bastnasite. There was no systematic study on reaction mechanism, products composition and thermal dynamic calculation of the calcination procedure of the bastnasite. The thermal decomposition behaviour of natural bastnasite crystal in calcination in air was studied systematicaly by diffrential thermal analysis (DTA), thermal gravity (TG), chemical analysis and X-ray diffraction analysis in present work.

2 EXPERIMENTAL METHOD

The bastnasite crystal was mined from Mianning, Sichuan province. It was pulverized and sieved to 300 ~ 320 mesh. The sample is pale brown after pulverization. Its chemical composition and rare earth distribution ratio are listed in Table 1 and Table 2 respectively.

Table 1 Chemical composition of bastnasite(%)

species	RE_2O_3	SiO_2	CaO	BaO	MgO
content	>70	2.941	0.346	0.186	0.063
species	Al_2O_3	MnO	Fe	F	CO_2
content	0.200	0.014	0.270	10.0	18.15

Table 2 Rare earth distribution ratio of bastnasite(%)

species	La_2O_3	CeO_2	Pr_6O_{11}	Nd_2O_3	Sm_2O_3	Eu_2O_3	Gd_2O_3
ratio	27.5	49.92	4.5	14.0	1.25	0.25	0.58
species	Tb_4O_7	Dy_2O_3	Ho_2O_3	Er_2O_3	Yb_2O_3	Y_2O_3	
ratio	0.042	0.11	0.058	0.072	0.032	0.76	

A tubular resistance furnace was used in the experiment. The sample was heated with the furnace and cooled in the furnace. There were two types of atmosphere used in the experiment. They

① Received Jul. 19, 1993; accepted in revised form Nov. 12, 1993

were: (1) natural air, (2) dried air in which the water vapour was removed by two stages of sieve sorbent.

The DTA and TG experiments were carried out at a Shimazu BT-30 thermal analysis instrument and a Setaram MTb 10-8 instrument respectively. Their heating rate was 10 ℃/min. The XRD was carried out at a Rigaku D/Max-ra diffractometer, Cu K_α radiation was used.

3 RESULTS AND DISCUSSION

Fig. 1 is the thermal analysis curves of the bastnasite sample. From it we can see there is an endothermic peak in the DTA curve during 400～513 ℃. The temperature of the peak tip point is 480 ℃. An obvious weight lost happens during this temperature range in the corresponding TG curve. The total weight lost is 17.059%. It means at this temperature range the bastnasite decomposes because of heating and gives off CO_2.

Fig. 2 is the XRD patterns of the calcination products of the bastnasite at different temperature in natural air. From Fig. 2(1) we can see most part of the sample is (Ce, La) CO_3F with only a little impurities, such as α-SiO_2 etc. In Fig. 2(2), the diffraction peaks of the (Ce, La)CO_3F disappear completely. It means the (Ce, La)CO_3F has

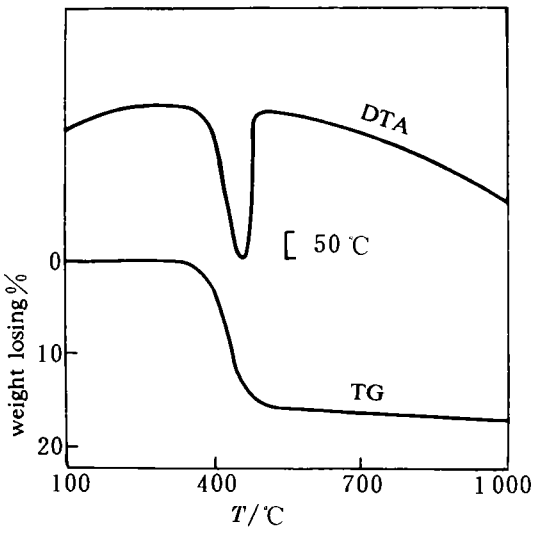

Fig. 1 DTA-TG curves of bastnasite

decomposed completely in this condition. The crystal structure of the prouduct is the same as that of (Ce, La)OF, both are FCC. But its peak positions shift to high angle side as compared with that of the (Ce, La)OF. This can be explained as part of F in the (Ce, La)OF is substituted by O. Because O is capable of absorbing one more electron than F, Ce^{3+} is oxidized into Ce^{4+} by the substituting O. Since the ion radius of the Ce^{4+} (92 pm) is smaller than that of the Ce^{3+} (103 pm), and the ion radius of O^{2-} (132 pm) is also smaller than that of F^- (133 pm), the crystal lattice constant and the distance between the diffraction planes become small when Ce^{3+} is oxidized to Ce^{4+}. This causes the diffraction peak positions to shift to the high angle side. It also means when (Ce, La)CO_3F decomposes, part of Ce is oxidized at the same time. The reaction product is (Ce, La)$O_{1+x}F_{1-x}$, where $0<x<1$. From Fig. 2 (2) we can also see the diffraction peaks of the (Ce, La)$O_{1+x}F_{1-x}$ widen obviously. It indicates the grain size of the crystal is very small[6]. Curve Fig. 2(3) is basically similar to Fig. 2 (2), but its peak width becomes rather narrower as compared with that in Fig. 2(2), and its peak positions shift to the high angle side farther. The (111) peak position shifts once more by 0.10° as compared with it in Fig. 2 (2) (see Fig. 3).

This indicates that the grain of the product coarsens and the F in the (Ce, La)$O_{1+x}F_{1-x}$ is farther substituted by O. At the same time the (Ce, La) $O_{1+x}F_{1-x}$ begins to decompose, and the Ce^{4+} and O^{2-} begin to enrich at some place. In Fig. 2 (4), the diffraction pattern changes apparently. The peaks of $CeLa_2O_3F_3$ are separated from the peaks of the (Ce, La)$O_{1+x}F_{1-x}$ and the remaining peaks shift to the high angle side farther. From Fig. 3 we can see the (111) peak of the (Ce, La) $O_{1+x}F_{1-x}$ shifts by approximately 0.62° as compared with that in Fig. 2(2). It indicates that the F in the (Ce, La)$O_{1+x}F_{1-x}$ is farther substituted by the O, and the d value of the (Ce, La)$O_{1+x}F_{1-x}$ is approching to the standard value of the CeO_2 gradually. The peaks of LaF_3 are also found in Fig. 2 (4). Its strongest peak is overlapped with the strongest peak of the (Ce, La)$O_{1+x}F_{1-x}$. In Fig. 2 (4), the peak width of the (Ce, La)$O_{1+x}F_{1-x}$ becomes smaller than that in Fig. 2(3), but it is still wide. This indicates that the grain has farther coars

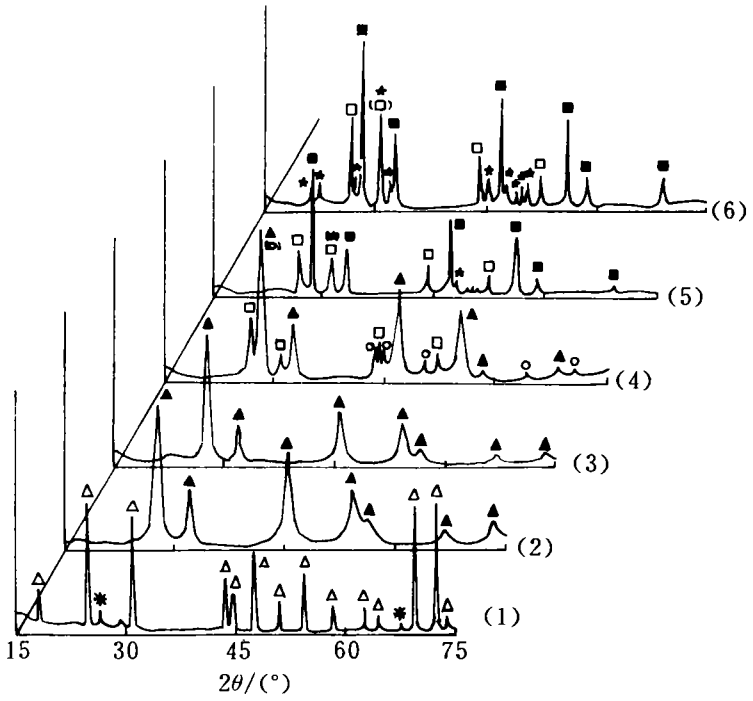

Fig. 2 XRD patterns of products of bastnasite in different calcination conditions in natural air

(1)—Raw material; (2)—400 C, 1h; (3)—500 C, 1h; (4)—700 C, 1h; (5)—1 000 C, 1h; (6)—1 000 C, 2h; △—$(Ce,La)CO_3F$; ＊—α-SiO_2; ▲—$(Ce,La)O_{1+x}F_{1-x}$; ◯—LaF_3; □—$CeLa_2O_3F_3$; ★—$Ca_1La_6(SiO_4)_6(OH)_2$; ■—CeO_2

ened, but it remains very fine. In Fig. 2(5), with the calcination temperature increasing, the $(Ce,La)O_{1+x}F_{1-x}$ is oxidezed completely into CeO_2, so, $x = 1$. Its (111) peak position shifts by 0.86° to the high angle side altogether as compared with that in Fig. 2(2), and its peak width decreases greatly. The peaks of the LaF_3 formed at lower temperature disappear, and the peaks of $Ca_1La_6(SiO_4)_6(OH)_2$ emerge. This means the LaF_3 can react with the impurities at high temperature. In Fig. 2(6), the peak positions of the CeO_2 change hardly with the increasing of the calcination time at 1 000 C. Only the relative peak intensity of the products changes slightly. The peak intensity of the $CeLa_2O_3F_3$ decreases while that of the $Ca_1La_6(SiO_4)_6(OH)_2$ and CeO_2 increases. This shows the $CeLa_2O_3F_3$ can be decomposed into CeO_2 and LaF_3 with the increasing of the calcination time at high temperature, then, the LaF_3 farther reacts with the impurities.

Repeated the Fig. 2(3)and (5) experiments in the flowing air dried by two stages of sieve sorbent. The XRD analysis results indicate that the calcination product gotten at 500 C in dry air is the same as that gotten in natural air, their XRD patterns are the same. In the XRD pattern of the products gotten at 1 000 C in dry air, the peak positions of the CeO_2 and $Ca_1La_6(SiO_4)_6(OH)_2$ do not change, but their intensity increases. The peaks of the $CeLa_2O_3F_3$ disappear completely while that of the LaF_3 appear again. This farther indicates that the small amount of water vapour existing in the air does not affect the bastnasite calcination. Because the flowing air can carry the gas which is emitted in the calcination away, and O can be supplied sufficiently at the same time, the decomposition of the $CeLa_2O_3F_3$ is accelerated by the flowing air, and the relative content of the CeO_2 and $Ca_1La_6(SiO_4)_6(OH)_2$ increases. Because of the limited content of the impurities, the peaks of the LaF_3 appear again in the XRD pattern. So during

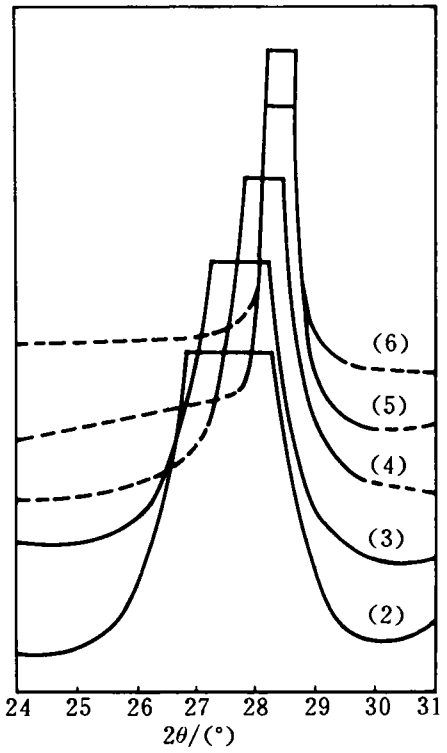

Fig. 3 Changes of (111) peak position of (Ce, La)$O_{1+x}F_{1-x}$ in calcination

(2)—400 C, 1 h; (3)—500 C, 1 h; (4)—700 C, 1 h; (5)—1 000 C, 1 h; (6)—1 000, 2 h

Only the bottom of (111) peaks are drawed in the figure; The positions of other peaks, which are omitted in the figure, are replaced by dashed lined for clarity

the thermal decomposition procedure of the bastnasite in air, the (Ce, La)CO_3F_3 is oxidized and decomposed to (Ce, La)$O_{1+x}F_{1-x}$ at first. Then with the calcination temperature and time increasing, the (Ce, La)$O_{1+x}F_{1-x}$ is farther oxidized and decomposed to CeO_2 and other rare earth compounds etc. The two procedures can be described by chemical equations as:

$$(Ce, La)CO_3F + O_2 \rightarrow (Ce, La)O_{1+x}F_{1-x} + CO_2 + F \quad (1)$$

$$(Ce, La)O_{1+x}F_{1-x} + O_2 \rightarrow CeO_2 + LaF_3 + CeLa_2O_3F_3 \quad (2)$$

Temperature and calcination time increasing farther, or in an oxygen-rich atmosphere, the $CeLa_2O_3F_3$ can be also decomposed to the CeO_2 and LaF_3. During the calcination procedure the amount of F in the samples decreases gradually.

The chemical analysis of the calcination products also shows the changes of the F content. The analysis results are shown in Table 3. Compared with the Table 1, the amount of Si in the samples calcined at 500 C or 1 000 C for 1 h respectively is higher than that in the bastnasite not to be calcined, but the amount of F is lower. It shows that the defluorination happens during the calcination process, but not for Si.

Table 3 Chemical analysis results of F and Si in calcination products

species	calcination 500 C, 1 h	condition 1 000 C, 1 h
SiO_2	5.52	5.28
F	9.5	6.0

The colour of the calcination products also changes with the different calcination temperature and time. From lower temperature to higher, 1 h to 2 h, the colour changes from pale brown to red-brown. Perhaps it is caused by the continuous changes of the products. Sintering phenomenon is also observed under the high temperature calcination. It becomes more prominent when the calcination temperature or time increases.

The thermal dynamics of the calcinaton procedure is calculated by using the DTA curve and the differential difference equation as:

$$\frac{\Delta \lg \Delta T}{\Delta \lg S''} = -\frac{E}{4.575}\left[\frac{\Delta(1/T)}{\Delta \lg S''}\right] + n \quad (3)$$

$$S'' = S - S' \quad (4)$$

Where T is the temperature of point D which is arbitrary point in the DTA curve, i. e. the abscissa; ΔT is the temperature difference of the point D, i. e. the ordinate; S is the total area under the DTA curve; S' is the area under the DTA curve between the point D and the point where the reaction starts; S'' is the difference between S and S'.

Plot $\Delta \lg \Delta T / \Delta \lg S''$ *vs* $\Delta(1/T) / \Delta \lg S''$, the activation energy E and the reaction order n can be obtained from the slope and intercept. The calculation results are shown in Fig. 4. The line equation obtained by least square fitting is

$$y = -10781.420x + 1.123 \quad (5)$$

So the activation energy E during the calcination process is 49.325 kJ/mol, and the reaction order n is 1.123.

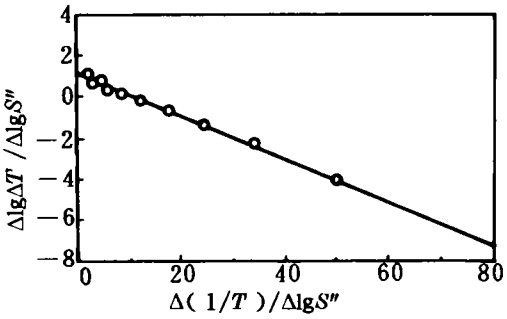

Fg. 4 Thermal dynamic calculation of decomposition of bastnasite by differential difference method

The relative coefficient $|r|$ is 0.996 which approches 1. It shows the y and x in the line equation have a good linear relationship.

4 CONCLUSIONS

(1) From the DTA-TG curves, bastnasite is decomposed by heating during 400～513 ℃ and discharges CO_2. The total weight lost is 17.059%.

(2) The thermal decomposition procedure of bastnasite in calcination in air can be seperated into two steps. At lower temperature, (Ce, La)CO_3F is oxidized and decomposed into (Ce, La)$O_{1+x}F_{1-x}$; Temperature and time increasing, (Ce, La)$O_{1+x}F_{1-x}$ is farther oxidized and decomposed into CeO_2 and $CeLa_2O_3F_3$ etc., i.e.

$$(Ce, La)CO_3F + O_2 \rightarrow (Ce, La)O_{1+x}F_{1-x} + CO_2 + F$$

$$(Ce, La)O_{1+x}F_{1-x} + O_2 \rightarrow CeO_2 + LaF_3 + CeLa_2O_3F_3$$

(3) With the increasing of calcination temperature and time, or in an oxygen-rich atmosphere, $CeLa_2O_3F_3$ can be farther decomposed into CeO_2 and LaF_3 etc.

(4) Part of F is lost during the calcination procedure, but not for Si.

(5) The colour of the calcination products changes from pale brown to red-brown with calcination temperature and time increasing. Sintering phenomenon is also observed under high temperature calcination.

(6) The activation energy E of the calcination procedure is 49.325 kJ/mol, and the reaction order is 1.123.

REFERENCES

1 Hirashima, Shiokawa. Journal of the Chemical Society of Japan, 1973, 3(3): 496.
2 Duncan, L K. US 3812233, 1974.
3 Zhang, C X; Ren, C Z; Li, C C; Tu, G F; Jin, M H. CN 1071205A, 1993.
4 Huang, B L. Handbook of Determination of Ores by Differential Thermal Analysis. Beijing: Scientific Press, 1987. 173.
5 Wang, Z W. Rare Earth, 1989, 1: 48.
6 Warren, B E. X-Ray Diffraction. Reading, Massachusetts: Addison-Wesley, 1969. Chapter 13.
7 Yu, B L; Jiang, J D. Practical Thermal Analysis. Beijing: Textile industry Press, 1990. 163.